The Auk 124(1):71–84, 2007

PHYLOGENETIC POSITION OF THE NEW WORLD QUAIL (ODONTOPHORIDAE): EIGHT NUCLEAR LOCI AND THREE MITOCHONDRIAL REGIONS CONTRADICT MORPHOLOGY AND THE SIBLEY-AHLQUIST TAPESTRY

W. Andrew Cox, Rebecca T. Kimball,[1] and Edward L. Braun

Department of Zoology, University of Florida, P.O. Box 118525, Gainesville, Florida 32611, USA

Abstract.—The evolutionary relationship between the New World quail (Odontophoridae) and other groups of Galliformes has been an area of debate. In particular, the relationship between the New World quail and guineafowl (Numidinae) has been difficult to resolve. We analyzed >8 kb of DNA sequence data from 16 taxa that represent all major lineages of Galliformes to resolve the phylogenetic position of New World quail. A combined data set of eight nuclear loci and three mitochondrial regions analyzed with maximum parsimony, maximum likelihood, and Bayesian methods provide congruent and strong support for New World quail being basal members of a phasianid clade that excludes guineafowl. By contrast, the three mitochondrial regions exhibit modest incongruence with each other. This is reflected in the combined mitochondrial analyses that weakly support the Sibley-Ahlquist topology that placed the New World quail basal in relation to guineafowl and led to the placement of New World quail in its own family, sister to the Phasianidae. However, simulation-based topology tests using the mitochondrial data were unable to reject the topology suggested by our combined (mitochondrial and nuclear) data set. By contrast, similar tests using our most likely topology and our combined nuclear and mitochondrial data allow us to strongly reject the Sibley-Ahlquist topology and a topology based on morphological data that unites Old and New World quail. *Received 3 April 2005, accepted 5 January 2006.*

Key words: Galliformes, incongruence, Odontophoridae, systematics.

Posición Filogenética de las Codornices del Nuevo Mundo (Odontophoridae): Ocho Loci Nucleares y Tres Regiones Mitocondriales Contradicen la Morfología y la Filogenia de Sibley y Ahlquist

Resumen.—La relación evolutiva entre las codornices del Nuevo Mundo (Odontophoridae) y otros grupos de Galliformes ha sido un área de debate. En particular, la relación entre Odontophoridae y Numidinae ha resultado difícil de resolver. Analizamos >8 kb de datos de secuencias de ADN de 16 taxa que representan todos los linajes principales de Galliformes para resolver la posición filogenética de Odontophoridae. Un conjunto de datos combinado de ocho loci nucleares y tres regiones mitocondriales analizado con métodos de máxima parsimonia, de máxima verosimilitud y Bayesianos apoya fuertemente la posición basal de Odontophoridae en un clado de fasiánidos que no incluye a los Numidinae. En contraste, las tres regiones mitocondriales presentan incongruencias modestas entre sí. Esto se refleja en los análisis de datos mitocondriales combinados, los cuales apoyan débilmente la topología de Sibley y Ahlquist, en la que Odontophoridae

[1]Address correspondence to this author. E-mail: rkimball@zoo.ufl.edu

ocupaba una posición basal con respecto a Numidinae y llevó a la decisión de reconocer a Odontophoridae como una familia aparte, hermana de Phasianidae. Sin embargo, pruebas de topología basadas en simulaciones hechas empleando los datos mitocondriales no pudieron rechazar la topología sugerida por nuestro conjunto de datos mitocondriales y nucleares combinados. En cambio, pruebas similares hechas utilizando nuestra topología más verosímil y nuestros datos nucleares y mitocondriales combinados nos permitieron rechazar fuertemente la topología de Sibley y Ahlquist y una topología basada en datos morfológicos que agrupa a las codornices del Viejo y del Nuevo Mundo.

The Order Galliformes contains many of the best-recognized and economically important avian species, such as the chicken, Japanese quail, turkey, and guineafowl. (Scientific names of species are listed in Table 1.) Reflecting their economic value in agriculture, the galliforms are well-studied avian taxa from the standpoint of genetics, genomics, and developmental biology (International Chicken Genome Sequencing Consortium 2004, Stern 2005). Four galliform families are currently recognized: Megapodidae (megapodes and brush turkeys), Cracidae (currassows and guans), Odontophoridae (New World quail), and the largest family, the Phasianidae, which includes the junglefowl (chickens), pheasants, partridges, Old World quail, grouse, turkey, and guineafowl (AOU 1998). Although the galliforms are very well studied in many ways, we still know little about evolutionary relationships within and among the galliform families.

The New World quail are morphologically and behaviorally distinct from the Phasianidae in many respects (e.g., Holman 1961, Johnsgard 1988) and, thus, form a unique group within the galliforms. In particular, the New World quail have a serrated lower mandible otherwise absent within the galliforms. Although many of the displays found within the New World quail are also found in other galliforms, the quail appear to lack a lateral waltz (or wing-droop) display that is common among the phasianids. The phylogenetic position of the New World quail has been much debated (e.g., Crowe 1988, Kornegay et al. 1993, Armstrong et al. 2001), and it is not clear whether the New World quail should form a family distinct from the phasianids or whether they are a unique monophyletic group nested within the phasianids.

Traditional classifications using morphological data place the New World quail in various positions within the phasianids (Fig. 1A, B; reviewed by Crowe 1988, Sibley and Ahlquist 1990, Dyke et al. 2003). A recent, large-scale cladistic analysis of morphological traits, for example, found that the New World quail were closely related to several genera of Old World quail and partridges (Dyke et al. 2003; e.g., Fig. 1B), united by the presence of a well-developed secondary *fossa pneumataicum* on the proximal end of the humerus. Similarly, Hudson et al. (1959) examined appendicular morphology of some galliforms and suggested that the similarity of sesamoids of the New World quail and partridges of the genus *Alectoris* was unlikely to be attributable to convergence. By contrast, DNA–DNA hybridization suggests that the New World quail form a lineage basal to the guineafowl and other phasianids (including partridges and Old World quail), as shown in Fig. 1C (e.g., Sibley and Ahlquist 1990). The DNA–DNA hybridization results, combined with the unique morphology of the New World quail (Holman 1961), led to placement of the New World quail in their own family, Odontophoridae, which is believed to be the sister group of the Phasianidae (American Ornithologists' Union [AOU] 1997).

Recent molecular work has not provided clear resolution on the relationship between the New World quail and phasianids. Several phylogenetic studies using mitochondrial cytochrome-*b* sequences have provided limited support for placement of the quail basal to the guineafowl (Kornegay et al. 1993, fig. 5b in Randi 1996, Kimball et al. 1999, Armstrong et al. 2001; Fig. 1C). Using some analytical methods, cytochrome *b* places quail together in a clade with guineafowl (fig. 5a in Randi 1996; Fig. 1D), which is consistent with lysozyme amino-acid sequences (Jollès et al. 1979) and a maximum-likelihood (ML) analysis of a combined mitochondrial 12S ribosomal RNA (12S) and NADH dehydrogenase subunit

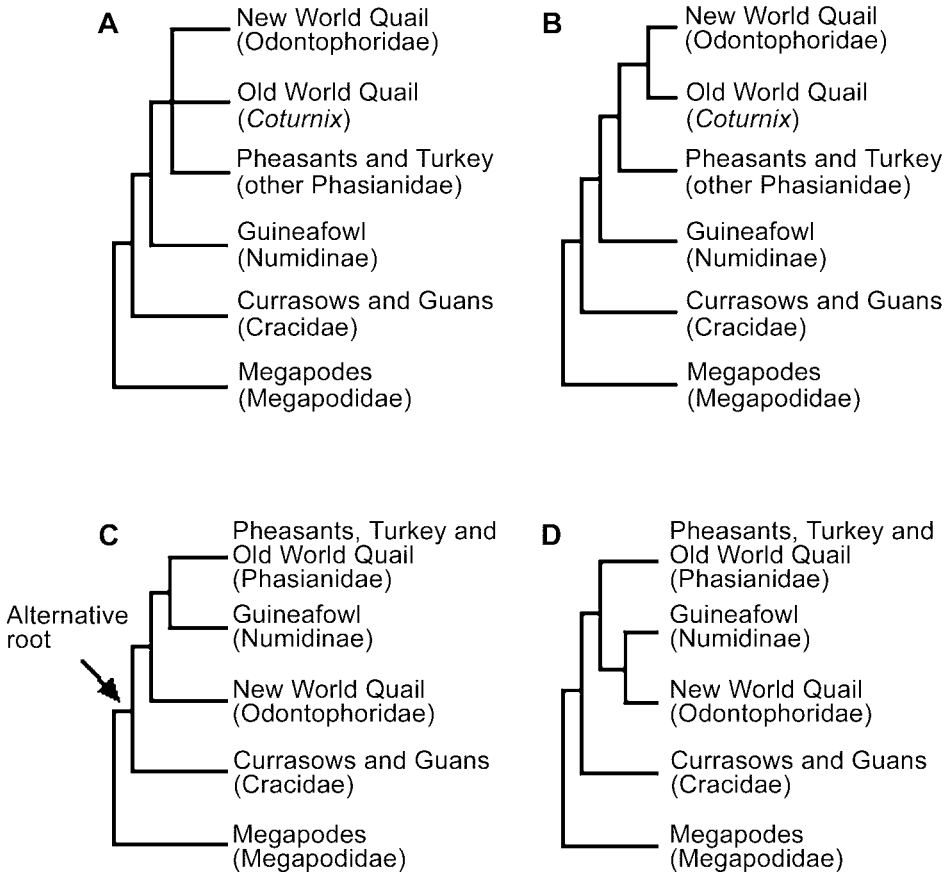

Fig. 1. Differing hypotheses about the phylogenetic position of the New World quail. (A) New World quail derived (e.g., OvoG topology from Armstrong et al. 2001). (B) New World quail derived and sister to Old World quail (e.g., Dyke et al. 2003). (C) New World quail basal in relation to guineafowl (e.g., Kimball et al. 1999, Sibley and Ahlquist 1990). Sibley and Ahlquist (1990) suggested an alternative rooting (see arrow) that forms a clade containing megapodes and cracids. (D) New World quail sister to guineafowl (e.g., fig. 5a in Randi 1996).

2 (ND2) data set (Dimcheff et al. 2002). By contrast, analyses of ovomucoid intron G (OvoG) nuclear sequences place New World quail as derived in relation to the guineafowl (Armstrong et al. 2001; Fig. 1A, B), as does parsimony analysis of the combined 12S and ND2 data set (Dimcheff et al. 2002; Fig. 1A).

Here, we attempt to overcome the poor resolution and conflicting results of previous molecular studies in galliforms by analyzing a relatively large set of DNA sequence data (8,653 total base pairs [bp]) from eight unlinked nuclear genes and three mitochondrial gene regions to examine the phylogenetic position of the New World quail. Our sample consists of 16 taxa, representing all major lineages of the four families of the Galliformes: Cracidae, Megapodidae, Odontophoridae, and Phasianidae (including the guineafowl). We use these molecular data to resolve the phylogenetic relationship between the New World quail and other galliform taxa, and we use simulation-based topology tests to assess the strength of our results.

Methods

DNA extraction, sequencing, and alignment.—We used a combination of previously published sequences as well as novel data that we generated ourselves (Table 1). Many

TABLE 1. Species and GenBank accession numbers for sequences used.

	AldB	BFib	Cal	DCoH	G3PDH	HMG	OvoG	Rhod	12S	ND2	CYB
Megapodes											
Alectura lathami	AY952663	AY952647	AY952679	AY952698	AY952714	AY952730	AY952767	AF394644	AY274004	AF394616	AF082058
Leipoa ocellata	AY952664	AY952648	AY952680	AY952699	AY952715	AY952731	AY952768	AF394647	AF222586	AF394618	AY952695
Megapodius layardi	AY952665	AY952649	AY952681	AY952700	AY952716	AY952732	AY952769	AF394657	AY952761	AF394635	AY952696
Cracids											
Crax rubra	AY952666	AY952650	AY952682	AY952701	AY952717	AY952733	AY952770	AY952750	AY274003	AY952746	AY956378
Ortalis vetula	AY952667	AY952651	AY952683	AY952702	AY952718	AY952734	AF170974	AY952751	AY952762	AF394614	L08384
Guineafowl											
Guttera pucherani	AY952668	AY952652	AY952684	AY952703	AY952719	AY952735	AY952771	AY952752	AY952763	AY952747	AY956379
Numida meleagris	AY952669	AY952653	AY952685	AY952704	AY952720	AY952736	AF170975	AF394642	AF222587	AF394613	L08383
New World Quail											
Colinus virginianus	AY952670	AY952654	AY952686	AY952705	AY952721	AY952737	AY952772	AY952753	AF222576	AF222545	AY952697
Cyrtonyx montezumae	AY952671	AY952655	AY952687	AY952706	AY952722	AY952738	AF170976	AY952754	AY952764	AY952748	AF068192
Oreortyx pictus	AY952672	AY952656	AY952688	AY952707	AY952723	AY952739	AF170977	AY952755	AY952765	AY952749	AF252860
Pheasants, Turkey, Old World Quail											
Coturnix japonica	AY952673	AY952657	AY952689	AY952708	AY952724	AY952740	AY952773	AY952756	AP003195	AP003195	L08377
Gallus gallus	AY952674	AY952658	AY952690	AY952709	AY952725	AY952741	AF170979	AY952757	X52392	X52392	AF028795
Pavo cristatus	AY952675	AY952659	AY952691	AY952710	AY952726	AY952742	AF170990	AF394640	AY952766	AF394612	L08379
Meleagris gallopavo	AY952676	AY952660	AY952692	AY952711	AY952727	AY952743	AF170984	AY952758	U83741	AF222556	L08381
Phasianus colchicus	AY952677	AY952661	AY952693	AY952712	AY952728	AY952744	AY952774	AY952759	U83742	AF222561	AF028798
Tragopan temminckii	AY952678	AY952662	AY952694	AY952713	AY952729	AY952745	AY952775	AY952760	AF222595	AF222566	AF028802

DNA samples came from individuals that we have used in previous studies (e.g., Kimball et al. 1999, Armstrong et al. 2001). Additional DNA samples included *Colinus virginianus* (provided by L. Krassnitzer), *Guttera pucherani* and *Crax rubra* (provided by T. M. Crowe), and all three Megapodidae (provided by S. Birks). Sample quantities of both *C. rubra* and *G. pucherani* samples were insufficient for polymerase chain reaction (PCR) amplification of all 11 loci, so each sample was subjected to whole-genome amplification using GENOMIPHI (Amersham Biosciences, Buckinghamshire, United Kingdom). To test for contamination in the whole-genome amplifications, the DNA samples amplified by GENOMIPHI were diluted and used as a template for PCR amplification of a gene region that had been amplified and sequenced from the original genomic DNA sample. The PCR products produced using the *C. rubra* and *G. pucherani* templates amplified by GENOMIPHI were sequenced. This sequence was compared with the existing sequence data for *C. rubra* and *G. pucherani*. For both species, samples amplified from genomic DNA gave identical sequences to those amplified from the DNA treated with GENOMIPHI.

To obtain data from additional species and for novel loci, we used a combination of previously published and newly designed primers (Table 2). The PCR products were cleaned by precipitation using an equal volume of PEG (20%):NaCl (2.5 M) or by Wizard SV Gel and PCR Cleanup Kit (Promega, Madison, Wisconsin). Cleaned PCR products were sequenced in forward and reverse directions with the primers used in PCR amplification. For some loci (cytochrome *b*, ND2, 12S, BFib, and Rhod), sequencing with additional internal primers (Table 2) was necessary to obtain double-stranded sequences. Cycle sequencing was performed using ABI BigDye Terminator, version 3.1 (Applied Biosystems, Foster City, California) or Beckman DTCS Quickstart kits (Beckman-Coulter, Fullerton, California). Sequences were obtained using an ABI Prism 3100-Avant genetic analyzer (Applied Biosystems) or a CEQ 8000 (Beckman-Coulter) genetic analysis system. Length polymorphisms between alleles in some nuclear loci resulted in unusable sequence data, so these PCR products were cloned using the pGEM-T Easy vector (Promega). In these cases, two plasmids were prepared for sequencing using the Eppendorf Perfectprep Plasmid Mini kit (Eppendorf North America, Westbury, New York) and sequenced using the same protocol that we used for PCR products.

Sequences were examined and assembled into double-stranded contigs using SEQUENCHER, version 4.1 (Gene Codes Corporation, Ann Arbor, Michigan). Sequences of the mitochondrial coding regions were equal in length and did not have any insertions or deletions, so alignment was straightforward. Nuclear sequences and the mitochondrial 12S region were initially aligned using CLUSTAL_X (Thompson et al. 1997). The aligned sequences were then imported into MACCLADE, version 4.0 (Maddison and Maddison 2000) and optimized by eye.

Phylogenetic analyses.—Multiple analyses were performed on each individual locus or gene region, on a combined mitochondrial partition, on a combined nuclear partition, and on a combined nuclear and mitochondrial data set. To determine whether the partitions represented different genealogical histories, we performed the partition homogeneity test (incongruence length difference test; Farris et al. 1995). We performed the test in two ways: (1) with each locus (or mitochondrial region) as a different partition and (2) comparing the mitochondrial with the nuclear partitions. We did each test (1) using all sites and (2) using only the informative sites. For each test, we used a heuristic search with 1,000 replicates and 10 random-sequence additions per replicate.

Maximum-parsimony (MP) and ML analyses were performed using PAUP*, version 4.0b10 (Swofford 2003). For MP bootstrap analyses, a heuristic search with 10 random additions was performed for each of 1,000 bootstrap replicates. For ML analyses, the appropriate model for each partition was determined by the hierarchical likelihood-ratio test in MODELTEST, version 3.06 (Posada and Crandall 1998). Support in ML analyses was examined using the bootstrap (500 replicates and the rapid ML algorithm implemented in PHYML, version 2.1b; Guindon and Gascuel 2003). Briefly, 500 bootstrapped data sets were generated using SEQBOOT from the PHYLIP package, version 3.6 (Felsenstein 2005); the ML tree for each bootstrapped data set was found using PHYML; and then a majority rule consensus tree was generated using CONSENSE from the PHYLIP package.

Table 2. Regions used for analyses. For each region, we have given location in the chicken genome (if known) and primer sequences used for amplification and sequencing.

Gene (abbreviation)	Location [a]	Intron(s)	Primer sequence (5′ to 3′)	Primer
Aldolase b (AlbB)	Z	6	GAGCCAGAAGTCTTACCTGAYGG	AldB6F
			CAGCTGTCACCATGTTNGG	AldB7R
Beta-fibrinogen (BFib)	4	7	GGAGAAAACAGGACAATGACAATTCAC	F1B-B17UF [b]
			TCCCCAGTAGTATCTGCCATTAGGGTT	F1B-B17LR [b]
			GTAATRCAGAGATGARTCCT	BFib7intF1
			CACTCCAGTAATACAGAGATGAGTCC	BFib7intF2
			TACTCATTATCAGAAACTGCTGGTGG	BFib7intF3
			CARTTCCYKCAGTTCATAATGA	BFib7intR1
			TCTCTTCCCTCAGGACCCATTTCT	BFib7intR2
Calbindin (Cal)	2	9, 10	AGGGTGTCAARATGTGTGSGAAAGA	Cal9F
			GTANAGCTTCCCTCCATCNGACAA	Cal11R
Dimerization cofactor of HNF1 (DCoH)	unknown	3	AGGCCTGGCTTCATGAC	DCOH3F
			GATAAACCYGTGCARTCYTGGGTGCT	DCOH4R
Glyceraldehyde 3-phosphate dehydrogenase (G3PDH)	1	11	TGCGGGTGCTGGCATTGC	G3PDH11F [b]
			TGCATGCCATGTGGACCAT	G3PDH11R
High mobility group 17 (HMG)	23	2, 3	GCTGAAGGAGATACCAARGGCGA	HMG172F
			CTTTGGAGCTGCCTTTTTAGG	HMG174R
Ovomucoid (OvoG)	13	G	CAAGACATACGGCAACAARTG	OVOGF [b]
			GGCTTAAAGTGAGAGTCCCRTT	OVOGR [b]
Rhodopsin (Rhod)	12	1	GAACGGGTACTTTGTCTTTGGAGTAAC	Rhod1F
			CCCATGATGGCGTGGTTCTCCCC	Rhod1R
			TGTGTCTGAGAACGGCCTCC	RhodintF
			GRGGAGGCCRTTCTCAGAC	RhodintR
12S ribosomal RNA (12S)	mitochondrial DNA		ACACAAAGCATGGCACTGAA	L1267 [b]
			CTTTCAGGTGTAAGCTGARTGCTT	H2294 [b]
			AAACTGGGATTAGTACCCCACTAT	L1753 [b]
			ATAGTGGGGTATCTAATCCCAGTTT	H1729 [b]
NADH dehydrogenase 2 (ND2)	mitochondrial DNA		GCCCATACCCCRAAAATG	L5216 [b]
			CCTTATTTAAGGCTTTGAAGGC	H6313 [b]
			CCCTACTYACCYTCCTAGCAAT	L5716
			GATGARAAGGCTAGGATYTTTCG	H5766

TABLE 2. Continued.

Gene (abbreviation)	Location [a]	Intron(s)	Primer sequence (5′ to 3′)	Primer
Cytochrome *b*	mitochondrial DNA		ATCGCCTCCCACCTRATSGA	L14731 [b]
			GCAAACGGCGCCTCATTCT	L15164 [b]
			AGGGTTGGTTGTCGACTGA	H15400 [b]
			CTAGGCGACCCAGAAAACTT	L15662 [b]
			CGGAAGGTTATGGTTCGTTGTTT	H15826 [b]
			TTCAGTTTTTGGTTTACAAGAC	H16065 [b]

[a] Chicken chromosome that contains the relevant locus.
[b] Primers previously published or modified: Friesen et al. (1997), Prychitko and Moore (1997), Kimball et al. (1999), Sorenson et al. (1999), Armstrong et al. (2001).

Bayesian analyses were conducted using MRBAYES, version 3.0b4 (Huelsenbeck and Ronquist 2001, Ronquist and Huelsenbeck 2003), using the best-fitting model implemented in that program. To ensure convergence of the Markov chain, we ran our chains for 2×10^7 generations and discarded the first 5×10^5 generations. The posterior probabilities for clades reported here reflect the proportion of trees sampled by the Markov chain that contain the clade of interest.

We considered nodes strongly supported when bootstrap values were >70% or when posterior probability values were >95% (e.g., Hillis and Bull 1993, Alfaro et al. 2003). We also showed nodes that received support in fewer than 50% of bootstrap replicates or posterior probability values of <0.5.

The most commonly used parametric test of topologies in phylogenetics (the SOWH test) was originally described by Swofford et al. (1996) and is explained in more detail by Goldman et al. (2000). The SOWH test examines the hypothesis that the observed data could have been generated by a specific tree with a likelihood lower than the ML tree (e.g., could the sequence data used to generate a total evidence tree with the New World quail derived in relation to guineafowl actually reflect sampling error for data generated on a tree similar to the Sibley-Ahlquist tapestry?). The suboptimal (e.g., tapestry) topology is used as a null hypothesis, and several data sets are simulated under this null hypothesis. Then, the ML tree for each of the simulated trees is identified, and the difference in –ln L likelihood values for the ML tree and null hypothesis tree is calculated (this test statistic is usually called δ). The null distribution of δ, calculated from these Monte Carlo simulations, can be used to estimate the probability that the observed data could have actually been generated on a tree like the null hypothesis tree. Buckley (2002) showed that parametric tests like the SOWH test can overestimate the support for incorrect topologies when the model is misspecified, so it is imperative to use the best-fitting model possible. Therefore, each nuclear locus or mitochondrial gene region was simulated separately using ML estimates of parameters for those gene segments in the evolver program from the PAML package, version 3.14 (Yang 1997) and concatenated to generate each simulated data set (mitochondrial protein-coding regions were

also broken into first, second, and third codon positions, because of the well-known differences in base composition among these positions; e.g., Kornegay et al. 1993). The ML tree searches were conducted using PHYML (Guindon and Gascuel 2003), and likelihoods for both the best tree and the null hypothesis tree were calculated using PAUP*. This strategy allowed us to combine the rapid tree search of PHYML with the use of specific features in PAUP* to effectively analyze the data in a computationally feasible manner. Shell scripts and C++ source code used to perform this analysis are available on request from E.L.B.

Several specific topologies were tested. Using the combined (mitochondrial plus nuclear) data set, we compared our best topology (e.g., Fig. 1A) with two alternatives represented by Figures 1B and 1C. We also used just the nuclear data with the alternative topology of quail basal (Fig. 1C). Finally, using the mitochondrial data, we compared the ML tree from the combined mitochondrial data with the ML tree obtained when we analyzed the total data set.

We used two different methods to estimate divergence times from the combined data set, a point calibration and a Bayesian approach. Because a likelihood-ratio test (Felsenstein 1988) suggested the data were not evolving in a clock-like manner (dln = 259.23, df = 14, $P <$ 0.001), our point calibrations were done using branch lengths estimated by nonparametric rate smoothing (Sanderson 1997) as implemented in TREE EDIT, version 1.0a10 (Rambaut and Charleston 1999), with the "weight rate difference at root with mean" option. For the Bayesian estimation, we used the approach of Thorne and Kishino (2002) as implemented in MULTIDIVTIME, with parameter estimates from PAML (Yang 1997). We used two fossils to calibrate our divergence times: the ~52 Ma *Gallinuloides*, which diverged before the separation of guineafowl from other phasianids (Dyke 2004), and the ~35 Ma *Schaubortyx* (Brodkorb 1964), which is a crown member of the *Gallus* and *Coturnix* clade (van Tuinen and Dyke 2004).

Results and Discussion

Molecular evolution of different gene regions.— Our final alignment had 8,653 bp (after excluding a 579-bp insertion in BFib unique to *Oreortyx pictus*). This included 5,439 bp of nuclear DNA and 3,214 bp of mitochondrial sequence data (Table 3). The nuclear data, when combined, contained a higher percentage of variable sites (47.9%) than the mitochondrial data (43.6%), though the mitochondrial data had a slightly greater percentage of parsimony-informative sites (Table 3).

Table 3. Comparison of the different nuclear loci and mitochondrial regions.

Locus	Length (% exon)	Variable (%)	Parsimony informative (%)	CI (excl. uninf.) [a]	Best model	ti/tv	alpha
AldB	510 (0)	47.8	27.5	0.752	HKY	1.93	N.A.
Bfib [b]	984 (0)	48.3	31.1	0.769	HKY+G	1.81	3.66
Cal	533 (14)	33.8	18.9	0.822	HKY+G	1.87	1.20
DCoH	585 (0)	46.7	27.2	0.737	K80+I	1.85	N.A.
G3PDH	414 (0)	46.9	30.4	0.730	HKY+G	1.91	1.82
HMG	763 (4)	57.3	40.9	0.698	HKY+G	2.41	1.51
OvoG	593 (0)	34.7	21.2	0.794	TIM+G [c]	1.93	1.82
Rhod	1,057 (0)	56.3	43.1	0.733	HKY+G	2.13	2.35
All nuclear	5,439 (2)	47.9	31.7	0.737	HKY+G	2.01	1.67
12S	1,030 (0)	36.1	26.3	0.481	GTR+I+G	4.59	0.49
ND2	1,041 (100)	52.1	40.9	0.458	GTR+I+G	6.06	0.98
Cytochrome *b*	1,143 (100)	42.7	33.2	0.445	GTR+I+G	6.58	0.52
All mtDNA [d]	3,214 (68)	43.6	33.5	0.455	GTR+I+G	4.98	0.71
Nuclear + mtDNA	8,653 (25)	46.3	32.4	0.581	GTR+I+G	2.41	0.76

[a] Consistency index calculated after excluding uninformative sites.

[b] BFib results exclude a unique 579 bp insertion in *Oreortyx pictus*.

[c] Because TIM + G was not implemented in MRBAYES or PHYML, GTR + G was used for Bayesian and ML bootstrap analyses.

[d] mtDNA = mitochondrial DNA.

The nuclear and mitochondrial data both showed marked variation among loci in the percentage of variable and parsimony-informative sites. Among nuclear loci, the partition with the greatest proportion of exon data (Cal) had the lowest percentage of variable and parsimony-informative sites. However, most nuclear loci had little or no exon data, yet still showed a large range in variability (e.g., OvoG had 34.7% variable sites, whereas Rhod had 56.3%, yet both contained no exon data). As might be expected, loci with a high percentage of variable sites also had a high percentage of parsimony-informative sites (and vice versa; Table 3). The mitochondrial partitions also showed differing levels of variation, with the two coding partitions differing by ~10% (Table 3)

The consistency index (calculated after excluding uninformative sites) was always higher for the nuclear loci than for the mitochondrial data (Table 3), which suggests that the nuclear loci exhibit less homoplasy than the mitochondrial data (e.g., Prychitko and Moore 1997, Armstrong et al. 2001). As expected from the overall rate of sequence evolution, the nuclear locus with the greatest consistency index was Cal, which (as stated above) also contained the greatest percentage of exon data. However, although there is some variation in apparent rates of evolution and degree of homoplasy among the nuclear loci, the amount of variation among the nuclear loci (or among the mitochondrial regions) was much less than that between the nuclear and mitochondrial partitions (Table 3).

In general, relatively simple models of sequence evolution exhibited good fits to the data on the basis of the hierarchical likelihood-ratio test for the nuclear loci, whereas more parameter-rich models were necessary to fit the mitochondrial gene regions (Table 3). In fact, the most complex model tested (GTR + G + I) was necessary to fit all three mitochondrial regions (as well as the complete mitochondrial alignment) on the basis of the hierarchical likelihood-ratio test. This raises the question of whether even more parameter-rich models will exhibit even better fit to the data for the mitochondrial DNA (mtDNA) regions. By contrast, the fact that less-complex models exhibited adequate fit to the nuclear data suggests that the models used here represent reasonable approximating models for the data. The same model was used for both ML and Bayesian analyses, with the exception of the OvoG locus (its best-fitting model for ML analyses is not implemented in MRBAYES). Results from MP, ML, and Bayesian models were congruent for each locus, though in some cases a particular analytical method was unable to provide support for specific relationships via the bootstrap or posterior probabilities for specific relationships.

The partition-homogeneity test did not reveal significant differences between partitions when we tested each locus as a different partition ($P_{\text{all sites}} = 0.184$, $P_{\text{informative sites}} = 0.211$) or when we compared the nuclear and mitochondrial partitions ($P_{\text{all sites}} = 0.289$, $P_{\text{informative sites}} = 0.286$). On the basis of these results, we concluded that the phylogenetic signals present in each locus or gene region were similar enough to combine for phylogenetic analyses.

Phylogenetic position of the New World quail.—The combined data set showed strong support for the hypothesis that the New World quail are derived in relation to guineafowl (Fig. 2), particularly when using Bayesian and ML analyses. However, none of the nuclear loci or mitochondrial regions (combined or individually) supported uniting the New and Old World quail, contrary to some conclusions from analysis of morphological data (e.g., Dyke et al. 2003). Similarly, the combined nuclear partition provided strong support for placing the New World quail as derived in relation to the guineafowl in all analytical methods. Six of eight nuclear loci are consistent with the combined nuclear topology in showing that the New World quail are derived in relation to guineafowl (Figs. 1A and 2). Of these six loci, support for this topology was strong for some loci but weak for others (Table 4). The two loci (Cal and HMG) that conflict with the hypothesis that the quail occupy a derived position in relation to the guineafowl supported different topologies using different analytical methods, and thus do not provide strong support for any particular hypothesis.

Results from the mitochondrial partitions were less clear, with greater differences among partitions than among types of analyses. For example, ND2 showed support for a basal position of the quail (e.g., Fig. 1C), 12S supports a topology consistent with most nuclear loci, and cytochrome *b* does not provide support for any specific position for the New World quail (Table 4). Results of the combined mitochondrial partition reflect

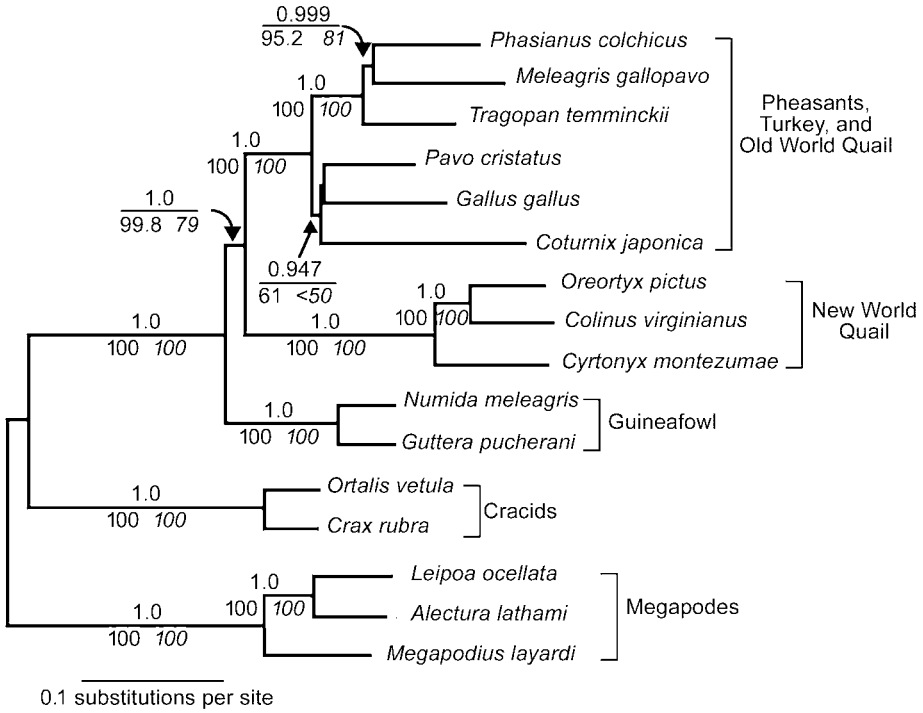

FIG. 2. Maximum-likelihood phylogeny of the total (nuclear plus mitochondrial) data set. Numbers at nodes represent proportion of posterior probability values from Bayesian analyses (above), percentage of ML bootstrap (below, left), and percentage of MP bootstrap (in italic, below, right).

TABLE 4. Results of phylogenetic analyses using different methods for each data partition. Values in bold indicate strongly supported results.

	Analytical method		
Locus	Parsimony [a]	ML bootstrap [a]	Bayesian [a]
AldB	**A (83)**	**A (72)**	A (0.84)
BFib	**A (97)**	**A (100)**	**A (1.00)**
Cal	C (68)	X	C (0.62)
DCoH	X	A (66)	A (0.92)
G3PDH	**A (79)**	**A (92)**	**A (0.96)**
HMG	**C (70)**	**C (76)**	X
OvoG	A (58)	A (68)	A (0.90)
Rhod	A (57)	A (58)	A (0.60)
All nuclear	**A (94)**	**A (100)**	**A (1.00)**
ND2	**C (90)**	C (64)	C (0.93)
12S	A (52)	**A (90)**	**A (0.96)**
Cytochrome *b*	A (52)	X	X
All mitochondrial DNA	C (57)	X	C (0.55)
Nuclear + mitochondrial DNA	**A (79)**	**A (100)**	**A (1.00)**

[a] Letters refer to topologies shown in Figure 1: A = quail derived in relation to guineafowl; C = quail basal in relation to guineafowl; X = neither position was supported at 50% bootstrap or posterior probability values (see also Fig. 1).

the incongruence between the mitochondrial regions, providing only weak support for placing the New World quail in a basal position in relation to the guineafowl (Table 4).

Though our mitochondrial data weakly support the position of the New World quail suggested by Sibley and Ahlquist (1990; Fig. 1C), a SOWH test using the mitochondrial data was unable to reject the hypothesis supported by both the nuclear and combined data set (Table 5). This suggests that the mitochondrial data do not have sufficient historical signal to resolve the phylogenetic position of the New World quail. By contrast, our nuclear data were able to reject the Sibley and Ahlquist topology, which suggests that the nuclear data have greater power to differentiate among alternative hypotheses regarding the position of the New World quail. Using the combined nuclear and mitochondrial data, our ML tree (e.g., Fig. 2) was significantly better than a topology uniting the Old and New World quails (Fig. 1B) as well as the Sibley and Ahlquist (1990) topology (Fig. 1C). Thus, the strong support in our analyses (Fig. 2) and our ability to reject each of the alternative hypotheses strongly suggest that the New World quail are basal members of a phasianid clade that excludes the guineafowl, contrary to current classification.

We used a molecular clock to examine the timing of the divergence of the New World quail from the other phasianids. Nonparametric rate-smoothing provided divergence time estimates of 47.7 and 48.6 mya (using *Schaubortyx* and *Gallinuloides*, respectively). A multilocus Bayesian approach calibrated with both fossils suggested a more recent divergence, placing the New World quail divergence ~41.1 mya (with a 95% confidence interval of 39.2–43.6 my). These values are more recent than the estimates of Pereira and Baker (2006), who also used the Bayesian approach but suggested divergences that were >60 mya. However, their estimates relied on mitochondrial data that placed the New World quail in a more basal position than that suggested by our analyses, though it is not clear whether that is sufficient to explain all of the difference in our divergence estimates. Regardless, the New World quail have been an isolated lineage for ≥40 my, which explains the many unique attributes of this group.

Although the data largely support the same position for the New World quail, there are clearly some data partitions that are incongruent with this hypothesis. In principle, these differences could reflect differences between gene trees and species trees (Maddison 1997) because of factors such as lineage sorting or ancient hybridization. The branch between the divergence of the guineafowl and the New World quail is relatively short (e.g., Fig. 2). However, our molecular-clock results suggest that this branch is between 1.4 (estimated using MULTIDIVTIME) and 3.3 mya (point calibrations), which is sufficiently long that lineage sorting is unlikely to explain our results. For example, explaining the two incongruent topologies for eight nuclear loci sampled would require us to postulate that the effective population size of the ancestral population that split into the guineafowl, New World quail, and phasianids was about 2.6×10^5 (using a branch length of 1.4 my) to 1.2×10^6 [using a branch length of 3.3 my; Nei 1987), and that this effective population size was maintained during the entire period over which ancestral polymorphisms would have to have been maintained. These large effective population sizes are more

Table 5. Results of the SOWH test for the position of the New World quail.

Data	Null hypothesis [a]	Observed δ [b]	$\delta_{critical}$ [c]	Maximum δ [d]	P_{obs} [e]
Mitochondrial data	A	0.180	2.558	10.494	0.31
Nuclear data	C	12.407	1.498	7.899	<0.002
All gene regions	B	193.641	0.952	8.092	<0.002
	C	17.979	0.959	4.195	<0.002
	D	18.524	2.680	5.796	<0.002

[a] Letters refer to topologies shown in Figure 1.

[b] Difference in *ln L* scores for the null hypothesis tree and the ML tree for the observed data.

[c] The value that δ must exceed to be significant with a type I error rate of 5%.

[d] Maximum value of δ observed for a total of 500 simulations. If the observed value of δ exceeds this value, the probability of observing such an extreme value of δ by chance is <0.002.

[e] Probability of the observed value of δ given that the true tree is the null hypothesis tree.

than an order of magnitude greater than estimates of long-term effective population sizes for abundant extant taxa (Moore 1995).

An alternative explanation for the estimates of phylogeny obtained for a subset of loci that place the New World quail basal to the guineafowl (Fig. 1C) would be that this position is driven by homoplasy that has created erroneous phylogenetic signal. If this is the case, we would postulate that our inability to adequately model the evolution of those loci has led to erroneous conclusions. We favor this explanation, because the support for placing New World quail basal to the guineafowl was generally lower when parametric (ML or Bayesian) approaches were used. This suggests that the underlying history of each gene region may be congruent and that the apparent incongruence is driven by errors in our estimates of phylogeny. If this is the case, the use of better approximating models (once developed) may result in congruent phylogenies for all gene regions.

Of particular interest are the incongruent results obtained from the mitochondrial regions. The mitochondrion is maternally inherited as a single region, and avian mitochondria do not appear to recombine (e.g., Berlin et al. 2004). Thus, the incongruence we observed between the ND2 and 12S regions is likely attributable to homoplasy rather than hybridization or lineage sorting. The complex molecular evolution of the mitochondrial partitions, and the possibility that more parameters will be needed to adequately model these regions, further suggest that homoplasy or erroneous phylogenetic estimation have led to incongruence in this partition.

Conclusions

Although the galliforms have been well studied in many ways, the evolutionary relationships among the major lineages within this group have been difficult to elucidate. The position of the New World quail has been one of the most intriguing problems in galliform evolution because analyses of morphology, DNA–DNA hybridization data, and nucleotide sequence data have provided very different conclusions (e.g., Crowe 1988, Sibley and Ahlquist 1990, Kornegay et al. 1993, Dyke et al. 2003). However, the relatively large set of sequence data collected for the present study provides strong (and mostly congruent) support for placing the New World quail derived in relation to the guineafowl (Fig. 2). Thus, we first suggest that osteological similarities between New and Old World quail (Hudson et al. 1959, Dyke et al. 2003) are likely attributable to convergence. Second, we suggest that the current taxonomic status of the New World quail and guineafowl is inaccurate and recommend that either the quail be placed as a basal member of the Phasianidae, or that guineafowl be removed from Phasianidae and placed in a family (Numididae) basal to Odontophoridae. Finally, we suggest that because some of our gene trees do not appear to accurately reflect the species tree, future suprageneric phylogenetic studies will benefit from incorporating multiple loci exhibiting different characteristics.

Acknowledgments

Helpful suggestions by B. Burkley, J. Chojnowski, J. Kirchman, and two anonymous reviewers greatly improved earlier versions of this manuscript. This research was facilitated by funding from the National Science Foundation (DEB-0228682) to R.T.K., E.L.B., and D. W. Steadman.

Literature Cited

Alfaro, M. E., S. Zoller, and F. Lutzoni. 2003. Bayes or bootstrap? A simulation study comparing the performance of Bayesian Markov chain Monte Carlo sampling and bootstrapping in assessing phylogenetic confidence. Molecular Biology and Evolution 20:255–266.

American Ornithologists' Union. 1997. Forty-first supplement to the American Ornithologists' Union *Check-list of North American Birds*. Auk 114:542–552.

American Ornithologists' Union. 1998. Check-list of North American Birds, 7th ed. American Ornithologists' Union, Washington, D.C.

Armstrong, M. H., E. L. Braun, and R. T. Kimball. 2001. Phylogenetic utility of avian ovomucoid intron G: A comparison of nuclear and mitochondrial phylogenies in Galliformes. Auk 118:799–804.

Berlin, S., N. G. C. Smith, and H. Ellegren. 2004. Do avian mitochondria recombine? Journal of Molecular Evolution 58:163–167.

Brodkorb, P. 1964. Catalogue of fossil birds: Part 2 (Anseriformes through Galliformes). Bulletin of the Florida State Museum 8: 195–335.

Buckley, T. R. 2002. Model misspecification and probabilistic tests of topology: Evidence from empirical data sets. Systematic Biology 51:509–523.

Crowe, T. M. 1988. Molecules vs. morphology in phylogenetics: A non-controversy. Transactions of the Royal Society of South Africa 46:317–334.

Dimcheff, D. E., S. V. Drovetski, and D. P. Mindell. 2002. Phylogeny of Tetraoninae and other galliform birds using mitochondrial 12S and ND2 genes. Molecular Phylogenetics and Evolution 24:203–215.

Dyke, G. J. 2004. The fossil record and molecular clocks: Basal radiations within the Neornithes. Pages 263–277 *in* Telling the Evolutionary Time: Molecular Clocks and the Fossil Record (P. C. J. Donoghue and M. P. Smith, Eds.). CRC Press, Boca Raton, Florida.

Dyke, G. J., B. E. Gulas, and T. M. Crowe. 2003. Suprageneric relationships of galliform birds (Aves, Galliformes): A cladistic analysis of morphological characters. Zoological Journal of the Linnean Society 137:227–244.

Farris, J. S., M. Källersjö, A. G. Kluge, and C. Bult. 1995. Testing significance of incongruence. Cladistics 10:315–319.

Felsenstein, J. 1988. Phylogenies from molecular sequences: Inference and reliability. Annual Review of Genetics 22:521–565.

Felsenstein, J. 2005. PHYLIP (phylogeny inference package), version 3.6. Distributed by the author. [Online.] Available at evolution.gs.washington.edu/phylip.html.

Friesen, V. L., B. C. Congdon, H. E. Walsh, and T. P. Birt. 1997. Intron variation in Marbled Murrelets detected using analyses of single-stranded conformational polymorphisms. Molecular Ecology 6:1047–1058.

Goldman, N., J. P. Anderson, and A. G. Rodrigo. 2000. Likelihood-based tests of topologies in phylogenetics. Systematic Biology 49:652–670.

Guindon, S., and O. Gascuel. 2003. A simple, fast, and accurate algorithm to estimate large phylogenies by maximum likelihood. Systematic Biology 52:696–704.

Hillis, D. M., and J. J. Bull. 1993. An empirical test of bootstrapping as a method for assessing confidence in phylogenetic analysis. Systematic Biology 42:182–192.

Holman, J. A. 1961. Osteology of living and fossil New World quails (Aves, Galliformes). Bulletin of the Florida State Museum 6: 131–233.

Hudson, G. E., P. J. Lanzillotti, and G. D. Edwards. 1959. Muscles of the pelvic limb in galliform birds. American Midland Naturalist 61:1–67.

Huelsenbeck, J. P., and F. Ronquist. 2001. MRBAYES: Bayesian inference of phylogenetic trees. Bioinformatics 17:754–755.

International Chicken Genome Sequencing Consortium. 2004. Sequence and comparative analysis of the chicken genome provide unique perspective on vertebrate evolution. Nature 432:695–716.

Johnsgard, P. A. 1988. The Quails, Partridges, and Francolins of the World. Oxford University Press, Oxford, United Kingdom.

Jollès, J., I. M. Ibrahimi, E. M. Prager, F. Schoentgen, P. Jollès, and A. C. Wilson. 1979. Amino acid sequence of pheasant lysozyme. Evolutionary change affecting processing of prelysozyme. Biochemistry 18:2744–2752.

Kimball, R. T., E. L. Braun, P. W. Zwartjes, T. M. Crowe, and J. D. Ligon. 1999. A molecular phylogeny of the pheasants and partridges suggests that these lineages are not monophyletic. Molecular Phylogenetics and Evolution 11:38–54.

Kornegay, J. R., T. D. Kocher, L. A. Williams, and A. C. Wilson. 1993. Pathways of lysozyme evolution inferred from the sequences of cytochrome *b* in birds. Journal of Molecular Evolution 37:367–379.

Maddison, D. R., and W. P. Maddison. 2000. MACCLADE: Analysis of Phylogeny and Character Evolution, version 4.0. Sinauer Associates, Sunderland, Massachusetts.

Maddison, W. P. 1997. Gene trees in species trees. Systematic Biology 46:523–536.

Moore, W. S. 1995. Inferring phylogenies from mtDNA variation: Mitochondrial-gene trees versus nuclear-gene trees. Evolution 49: 718–726.

Nei, M. 1987. Molecular Evolutionary Genetics. Columbia University Press, New York.

Pereira, S. L., and A. J. Baker. 2006. A molecular timescale for galliform birds accounting for uncertainty in time estimates and

heterogeneity of rates of DNA substitutions across lineages and sites. Molecular Phylogenetics and Evolution 38:499–509.

Posada, D., and K. A. Crandall. 1998. MODELTEST: Testing the model of DNA substitution. Bioinformatics 14:817–818.

Prychitko, T. M., and W. S. Moore. 1997. The utility of DNA sequences of an intron from the β-fibrinogen gene in phylogenetic analysis of woodpeckers (Aves: Picidae). Molecular Phylogenetics and Evolution 8: 193–204.

Rambaut, A., and M. Charleston. 1999. TREE EDIT, version 1.0a10. University of Oxford, Evolutionary Biology Group, United Kingdom. [Online.] Available at evolve.zoo.ox.ac.uk.

Randi, E. 1996. A mitochondrial cytochrome *b* phylogeny of the *Alectoris* partridges. Molecular Phylogenetics and Evolution 6: 214–227.

Ronquist, F., and J. P. Huelsenbeck. 2003. MRBAYES 3: Bayesian phylogeneic inference under mixed models. Bioinformatics 19:1572–1574.

Sanderson, M. J. 1997. A nonparametric approach to estimating divergence times in the absence of rate constancy. Molecular Biology and Evolution 14:1218–1231.

Sibley, C. G., and J. E. Ahlquist. 1990. Phylogeny and Classification of Birds: A Study in Molecular Evolution. Yale University Press, New Haven, Connecticut.

Sorenson, M. D., J. C. Ast, D. E. Dimcheff, T. Yuri, and D. P. Mindell. 1999. Primers for a PCR-based approach to mitochondrial genome sequencing in birds and other vertebrates. Molecular Phylogenetics and Evolution 12:105–114.

Stern, C. D. 2005. The chick: A great model system becomes even greater. Developmental Cell 8:9–17.

Swofford, D. L. 2003. PAUP*: Phylogenetic Analysis Using Parsimony (*and other methods), version 4.0. Sinauer Associates, Sunderland, Massachusetts.

Swofford, D. L., G. J. Olsen, P. J. Waddell, and D. M. Hillis. 1996. Phylogenetic inference. Pages 407–514 *in* Molecular Systematics, 2nd ed. (D. M. Hillis, C. Moritz, and B. K. Mable, Eds.). Sinauer Associates, Sunderland, Massachusetts.

Thompson, J. D., T. J. Gibson, F. Plewniak, F. Jeanmougin, and D. G. Higgins. 1997. The CLUSTAL_X windows interface: Flexible strategies for multiple sequence alignment aided by quality analysis tools. Nucleic Acids Research 25:4876–4882.

Thorne, J. L., and H. Kishino. 2002. Divergence time and evolutionary rate estimation with multilocus data. Systematic Biology 51: 689–702.

van Tuinen, M., and G. J. Dyke. 2004. Calibration of galliform molecular clocks using multiple fossils and genetic partitions. Molecular Phylogenetics and Evolution 30:74–86.

Yang, Z. H. 1997. PAML: A program package for phylogenetic analysis by maximum likelihood. Computer Applications in the Biosciences 13:555–556.

Associate Editor: J. Klicka